

Deep Octree-based CNNs with Output-Guided Skip Connections for 3D Shape and Scene Completion

Peng-Shuai Wang
 Microsoft Research Asia
 penwan@microsoft.com

Yang Liu
 Microsoft Research Asia
 yangliu@microsoft.com

Xin Tong
 Microsoft Research Asia
 xtong@microsoft.com

Abstract

Acquiring complete and clean 3D shape and scene data is challenging due to geometric occlusion and insufficient views during 3D capturing. We present a simple yet effective deep learning approach for completing the input noisy and incomplete shapes or scenes. Our network is built upon the octree-based CNNs (O-CNN) with U-Net like structures, which enjoys high computational and memory efficiency and supports to construct a very deep network structure for 3D CNNs. A novel output-guided skip-connection is introduced to the network structure for better preserving the input geometry and learning geometry prior from data effectively. We show that with these simple adaptions — output-guided skip-connection and deeper O-CNN (up to 70 layers), our network achieves state-of-the-art results in 3D shape completion and semantic scene computation.

1. Introduction

Despite the rapid development in 3D capturing techniques, it is still challenging to acquire accurate and complete 3D shapes and scenes due to the interference by shape geometry, surface material, lighting conditions as well as the noise introduced in the capturing process. Therefore, recovering a complete and accurate 3D geometry from partial and noisy 3D inputs become an essential task in 3D acquisition.

3D completion is inherently an ill-conditioned problem. Many methods have been proposed to tackle this challenging problem based on different priors. Optimization-based methods [17, 1, 36] exploit the local geometry properties, *e.g.* smoothness of the local surface or volume, for 3D shape completion. Although these methods are able to fill small holes well, they cannot recover large missing regions. Matching-based methods [31, 29] reconstruct 3D shapes with the help of surfaces or parts found in a 3D shape database that best match the input partial shape. However, these methods are sensitive to noise and could fail if no similar shapes exist in the database. Recently, learning-based methods have been proposed for 3D

shape completion [11, 5, 39, 43, 46] and scene completion [32, 6, 49, 20, 40]. Inspired by the learning techniques on the image domain, many dedicated network structures, and various loss functions have been designed for learning a general yet compact latent space from 3D data to infer complete 3D geometry. However, their direct and naïve extension from 2D images to 3D voxels introduces high-memory cost and inefficient computation issues. Limited by this inefficient 3D representation, many existing 3D learning methods are still in a shallow network architecture and have not benefited from the power of *deep* layers, which proved extremely useful for 2D vision and NLP learning [8].

In this paper, we present a deep learning approach for 3D shape and scene completion. Taking a noisy and incomplete point cloud of a 3D shape or scene as input, our method represents the input with an efficient octree structure and predicts the complete output via deep octree-based CNNs with novel *output-guided skip connections*. Our deep octree-based CNNs are based on the O-CNN framework [38, 39] which is highly efficient both in memory and computation cost and makes deep layers possible. Our network design for 3D completion follows the U-Net structure [28], which consists of two deep residual networks [14] for encoding and decoding. The encoding network is defined on the input octree and transforms the input into a compact latent code, while the decoding network takes the latent code as input to infer the octree and detailed point cloud of the complete shape or scene. As the input and output octrees are different due to this complete task, not all features defined at one octree level of the decoding network can find the corresponding features at the same octree level of the encoding network. We propose output-guided skip connections that add skip connections between the generated octree node and its corresponding and existing octree node in the input octree only. This output-guided scheme well preserves the geometric information in the input and is robust to the input noise.

We evaluate the effectiveness of our approach in typical benchmarks of 3D shape completion and semantic scene completion tasks. Experiments show that our simple network design — efficient 3D representations based on octree, deep

layers, and output-guided skip connections, outperforms the existing approaches and achieves state-of-the-art results.

2. Related Work

3D shape completion Many traditional shape completion algorithms rely on geometric priors such as volume smoothness to fill holes. Poisson surface reconstruction [17, 18] is one of the representative methods. A few methods [30, 13, 31, 29, 35] fill the missing regions by synthesizing filling patches based on the geometry from the rest shape or a shape database.

Neural networks have been extensively used for shape completion. In general, voxel-based networks [45, 42], Octree-based and kd-tree networks [38, 39, 12, 26, 37, 19], Point-based networks [23, 25, 34], implicit function-based networks [22, 3, 21] are all suitable to be adapted for this task. Particularly, Dai *et al.* [5] propose a 3D-Encoder-Predictor network, which uses a voxel-based encoder-decoder network with skip connections to regress the missing geometry. Han *et al.* [11] propose to decompose the shape completion task into two steps: global shape inference and local geometry refinement. Cao *et al.* [2] cascade OctNet-based fully convolutional sub-networks [27] infer missing surface areas. Other existing works focus either on reducing the full supervision to weakly-supervision [33], employ the generative adversarial loss to improve the shape completion quality [44, 46], or use implicit function-based shape representation for shape completion [22, 21].

3D scene semantic completion Based on the observation that scene semantic segmentation and completion are tightly intertwined, Song *et al.* [32] propose SSCNets to solve these two problems simultaneously, which achieve superior performance than previous approaches [50, 7]. VVNets [10] combine 2D view-based CNNs and 3D volumetric CNNs, thus greatly reduce the training and inference cost. By utilizing sparse convolution [9], SGCNets [48] further improve the efficiency and performance for scene semantic completion. In our method, we combine the octree-based U-Net with ResNet blocks and the specially designed skip connections with deep layers, enabling a simple and effective solution.

Skip connections in deep learning In the U-Net structure [28], the features from the encoder are concatenated with the features in the decoder via skip connections for merging the spatial information from the encoder into the decoder directly. ResNet [14, 15], uses skip connections to add the features between two or three consecutive convolution layers, which greatly eliminates the gradient explosion/vanishing problems.

Different from the 2D image domain, for 3D shape completion with sparse 3D representations like octrees, the spatial locations of the input and output points are different.

To address this issue, we propose *output-guided skip connections*: skip connections are added only where there are output features. The output-guided skip connection not only reduces the complexity of the network but also connects the essential input and output features.

3. Network design

3.1. Network overview

Our 3D completion network is built upon the octree-based autoencoder [39]. Multiple ResNet blocks [14] are stacked in the network. The encoder and decoder are linked via our output-guided skip connections. The overall network architecture follows the U-Net design [28], as shown in Figure 1, the network details are present in Section 3.3.

Input and output The network takes octrees built from the incomplete point cloud as the input and the ground-truth point cloud as the target output. The point cloud can be from 3D scans or other 3D forms that can be discretized as a point cloud, such as the voxelized shape. We assume the point cloud is equipped with oriented normals, if not, we estimate normals from points.

O-CNN encoder and decoder To make our paper self-explanatory, we briefly introduce the octree-based encoder and decoder [39]. The O-CNN encoder takes the octree as input and constrains the CNN computation within the octree with the rule: *where there is an octree node, there is CNN computation*. After a series of octree-based CNN operations [38], the generated feature maps are processed and down-sampled, and flow along with the octree structure in a bottom-up manner. With the O-CNN decoder, the target octree is generated in top-down order. In each level of the octree, one shared prediction module (2-layer MLP) processes the features contained in each octree node and predicts whether this octree node is empty or not. If the node is predicted to be non-empty, it will be further subdivided, and the feature on this node is passed to its children via an octree-based deconvolution operator. This process is repeated recursively until the specified maximum octree depth is reached. In the finest octree level, a local planar patch is predicted at each non-empty octree node, *i.e.* the

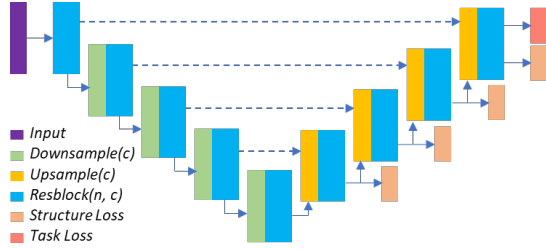


Figure 1: Our network architecture. c is the channel number. The input and output are octrees.

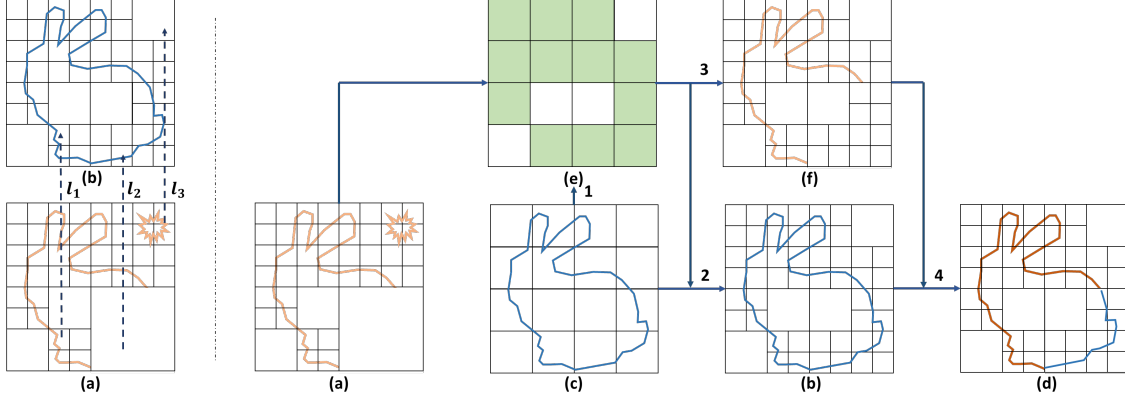


Figure 2: Output-guided skip connection. The left figures show three skip connections l_1 , l_2 and l_3 for analysis. Figures on the right show the construction of output-guided skip connections.

plane normal and displacement, are regressed as the final output.

3.2. Output-guided skip connections

When using octree-based autoencoders for shape completion, the input and output octree structures are different. The input octree is constructed from a partial shape which is even probably distorted by noise, while the desired output octree contains the complete shape. Due to this difference, the feature maps from the encoder are not aligned with the decoder, thus cannot be directly added via skip connections. We illustrate invalid alignments in Figure 2-left, where The input partial shape (a) contains additional noise on the top-right region and the ground-truth shape is in (b). Here we use 2D shapes and their corresponding quadtrees for illustration.

We analyze three possible skip connections denoted by l_1 , l_2 , and l_3 . We can see that l_1 is a valid skip connection since the corresponding input octree node contains information that needs to be retained in the output. l_2 is useless when the features on the input node are zero. l_3 is undesired since the features from the noise region should not be passed to the decoder, otherwise, they would interfere with the prediction.

To address the above issues, we propose *output-guided skip connections*. The basic idea is simple: the skip connection between the encoder and decoder is only added for a non-empty octree node in the output when there is an input octree node in the same location.

The output-guided skip connections are built as follows. Denote the feature map of octree level l in the decoder as D_l , the feature vector of an octree node with integer coordinate $\mathbf{x} = (x, y, z)$ as $D_l(\mathbf{x})$. The shared prediction module in octree level l takes $D_l(\mathbf{x})$ as input and predicts whether the octree node is empty or not. The output probability is rounded to 0 or 1 and denoted as $S_l(\mathbf{x})$. The octree nodes with $S_l(\mathbf{x}) = 1$ are further subdivided, and the coordinates of subdivided child octree nodes are $(2x + i, 2y + j, 2z + k)$ where $i, j, k \in \{0, 1\}$. Similarly, denote the octree node

feature of octree level l in the encoder as $E_l(\mathbf{x})$. Then the proposed skip connections can be formally defined as:

$$D_{l+1}(\mathbf{x}) = D_{l+1}(\mathbf{x}) + E_{l+1}(\mathbf{x}) \cdot S_l(\mathbf{x}/2). \quad (1)$$

Here $E_{l+1}(\mathbf{x}) = 0$ if there is no input octree node with coordinate \mathbf{x} . The arithmetic operation defined by Equation 1 is applied to every octree node and each channel of the feature map of the octree level $(l + 1)$ in the decoder respectively. It is possible to use the unrounded version of S_l in (1) in our network. Experiments show the benefit is margin, so we always use the rounded version for simplicity.

We illustrate the output-guided skip connection in Figure 2-right in which where one feature map of the encoder (a) is added to one feature map of the decoder (b) and the result is shown as (d). The overall operation includes 4 steps:

1. The prediction module of the decoder takes the features in (c) and predicts the node status as shown in (e), where the green color means the node is non-empty, *i.e.* $S_l(\mathbf{x}) = 1$;
 2. The octree in (c) is subdivided according to the status map (e);
 3. The features in (a) are multiplied with the mask of (e) and zeros are padded when the corresponding nodes do not exist in (a), the result is in (f);
 4. Features in (f) and (b) are added together and result in the feature map of (d).
- The dark yellow line in (d) is used for highlighting that the spatial information from (a) is added to (d). Note that the star shape, *i.e.* the outlier in the noisy input (a) can be easily filtered by the output-guided skip connection, which explains the robustness of our network to input noise conceptually.

The execution of output-guided skip connections is very efficient. The most expensive operation in Equation 1 is to search the octree node with the same coordinates for each octree node of the output octree. As the coordinates are stored as *shuffled keys* sorted in ascending order [41, 51], the searching operation can be executed efficiently via the parallel binary search operator provided by the Thrust library [16].

Remark OctNetFusion [26] proposes skip connections for OctNet [27] for the task of depth map fusion. However,

their skip connections are different from ours in nature. OctNetFusion uses skip connections to increase the receptive field by *statically* connecting feature maps from *the same octree structure*, whereas our skip connections are used to constrain the network focusing on the predicted shape by *dynamically* connecting feature maps from *the input and predicted octree structure*.

3.3. Network details

The details of all the layers in Figure 1 are as follows: $\text{conv}(c, k, s)$ is the octree-based convolution followed by BN and ReLU, where c is the number of output channel, k is the kernel size and s is the stride. $\text{Downsample}(c)$ is defined as $\text{conv}(c, 2, 2)$. $\text{Resblock}(n, c)$ is a stack of n ResNet blocks, each of which is made up of “ $\text{conv}(c/4, 3, 1) + \text{conv}(c, 3, 1)$ ” with skip connections between them. $\text{Upsample}(c)$: the octree-based deconvolution operator followed by BN and ReLU. The kernel size and stride are set as 2, and the output channel is c . In our experiments, c is set to 64 for the first $\text{Resblock}(n, c)$, increases by a factor of 2 after encountering each $\text{Downsample}(c)$, and decreases by a factor of 2 after every $\text{Upsample}(c)$. The upper bound of c is set to 256.

The prediction module of the decoder is a 2-layer MLP and outputs the probability of octree node status between 0 and 1 with a Sigmoid function as the final activation function. In the training stage, as the ground-truth octree node status is known, there is a sigmoid cross-entropy loss in each level of the octree, which is called as *Structure Loss*: L_{struct}^l , l is the level depth. In the finest level of the octree, *Task Loss*, denoted as L_{task} , are defined for different tasks. For shape completion (refer to Section 4.1), it has the following form: $L_{\text{task}} = \frac{1}{n} \sum (\|\mathbf{n} - \mathbf{n}^*\|^2 + |d - d^*|^2)$, where (\mathbf{n}, d) and (\mathbf{n}^*, d^*) are the predicted and ground-truth planar parameters contained in the finest non-empty octree node, respectively. For semantic scene completion (refer to Section 4.2), the network predicts the semantic labels of all non-empty voxels, so L_{task} is the multi-class cross-entropy loss. The total loss function of the network is defined as:

$$\text{Loss} = \sum_{l=3}^d L_{\text{struct}}^l + w \cdot L_{\text{task}}, \quad (2)$$

where d is the maximum octree depth, w is a weight factor and set to 1 in our experiments.

4. Experiments

We evaluate our networks on the tasks of 3D shape completion and semantic scene completion. We will release our code and models at <https://github.com/microsoft/O-CNN>.

4.1. 3D shape completion

For 3D shape completion, the incomplete input is a point cloud from single or multiple registered 3D scans. The goal

| | 3DEPN [5] | 3DRecGAN [46] | AE | <i>Our shallow</i> | <i>Our noise</i> | <i>Our deep</i> |
|--------------------|-----------|---------------|------|--------------------|------------------|-----------------|
| $D_c(\text{mean})$ | 8.63 | 5.37 | 5.80 | 3.47 | 3.44 | 3.06 |

Table 1: The statistics of the mean Chamfer distances – $D_c(\text{mean})$ on the shape completion task. All the shapes are normalized and centered in a box with size 128.

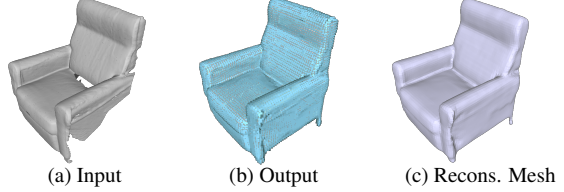


Figure 3: Shape completion on real data. The output points and reconstructed meshes are shown in column (b) and (c).

is to fill the missing regions.

Dataset We use the dataset provided by [5]. There are 26790 3D objects from 8 categories, 25,590 objects for training and 1,200 objects for testing. The partial scans are generated by virtual 3D scanning. Each object has been scanned 1 to 6 times from different views. These depth scans are back-projected into the original object space to form a point cloud and each point is assigned with a normal which is estimated from depth scans. We convert each incomplete point cloud to an octree of depth 6.

Implementation details As our output is an octree in which each finest leaf node contains a planar patch, we can sample multiple points on each patch and construct a point cloud. The approximation quality to the ground-truth complete point cloud is measured by using the discrete Chamfer distance metric. We set $n = 2$ for each Resnet block, resulting in a deep network with 51 layers. The training details are provided in supplementary materials.

Comparison We compared our method with state-of-the-art methods: 3D-Encoder-Predictor CNN (3DEPN) [5] and 3DRecGAN [46]. They take the partial TSDF [4] built from partial scans and regress the complete TSDF, with which the output mesh can be extracted. For evaluating the Chamfer distance, we sample dense points on the extracted mesh.

As deep layers and output-guided skip connections are the key components of our network, we also design alternative networks to justify their importance.

- *Shallow network*: *Our shallow*. We use a shallow network (14 layers) with a similar amount of trainable parameters to 3DEPN. The network is trained with the same training settings.
- *No skip connections*: *AE*. By removing the proposed skip connections, the network is essentially an octree-based autoencoder [39] with 51 layers.

The mean Chamfer distances of all the methods are summarized in Table 1. We observe the following facts:

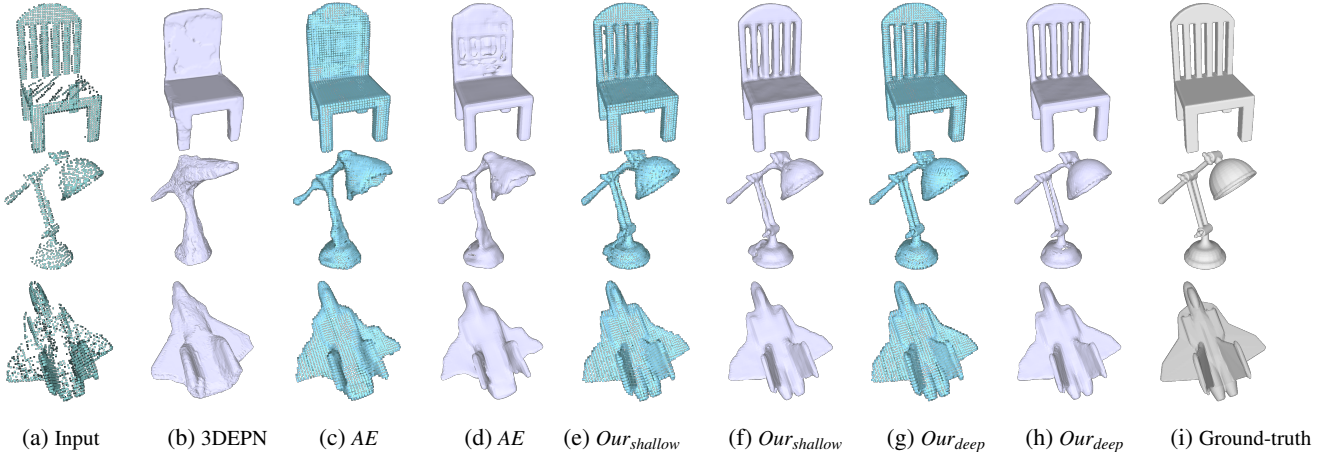


Figure 4: Visual comparison of single object completion. Figures in blue appearance are the *raw point clouds* produced by our networks. Figures in gray appearance are the reconstructed meshes. Apparently, our results (g) and (h) are much more faithful to the ground-truth.

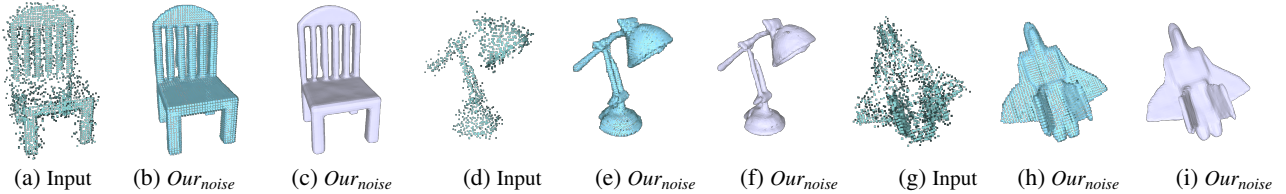


Figure 5: Robustness test of our network. The input noisy partial scans are in column (a), (d) and (g). The *raw output point clouds* are in column (b), (f) and (h). The reconstructed meshes are in column (c), (f) and (i). The ground-truth meshes are the same as those in Figure 4.

- Our deep and shallow network with output-guided skip connection outperform 3DEPN and 3DRecGAN significantly, which proves the superiority of combining octree with our proposed skip connections over volumetric TSDF with original skip connections everywhere. We explain this superiority is because our network constrains the CNN computation around the predicted surface and puts more focus on the predicted shape via output-guided skip connection, compared with 3DEPN and 3DRecGAN which have to predict all the voxels with high cost.
- Without skip connection, the performance of our deep network drops and is even worse than our shallow network with the skip connection. The completion results tend to be blurry and the geometric features are lost in some detailed regions as can be found in Figure 4. The result verifies that the spatial information contained in the input is essential and skip connection can well communicate this information for the completion task.

Robustness To verify the robustness of our network, we added Gaussian noise to the depth scan in the training dataset and train the network again with the same training settings. The mean of the Gaussian is set as 0, and the standard deviation is set as 2.5% of the width of the original object

bounding box. We denote this training network by *Our_{noise}*. From Table 1, we can see that the performance drops slightly compared with our deep network trained on clean data, but clearly better than other methods.

Result visualization We uniformly sample points with normals on the predicted octree and reconstruct the meshes via Poisson Reconstruction [18]. And the results are shown in Figure 4. The input partial scans and the ground-truth meshes are shown in column (a) and column (g).

It is clear to see that the geometric fidelity of results from our shallow network result (f) is much better than 3DEPN (b). With the deep network, the results are further enhanced and close to the ground-truth. As the deep autoencoder does not utilize the skip connection, its output quality is even worse than our shallow network, despite using deep layers.

We illustrate the completion results from noisy partial inputs in Figure 5. It can be seen that the output quality is high, and better than 3DEPN with clean partial scans and our AE, which verifies the robustness of our method.

We also tried our trained network on real scans as shown in Figure 3. The real data is provided by [24], which is scanned with a PrimeSense sensor. It can be seen our completion results are plausible.

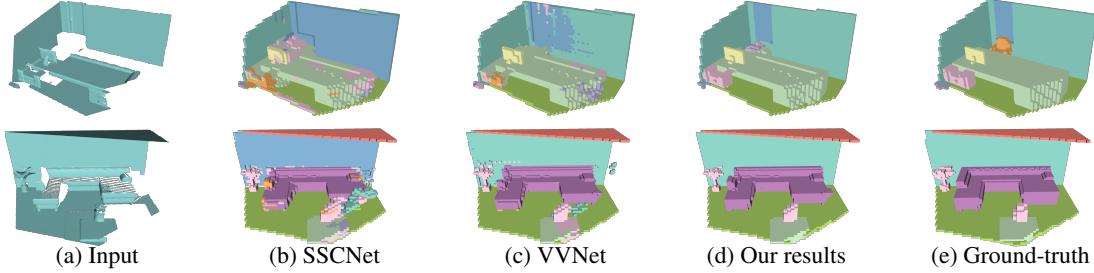


Figure 6: Visual results of semantic scene completion from one single depth image. Compared with SSCNet and VVNet, our results are much more faithful to the ground-truth.

| Method | Scene completion | | | Semantic scene completion | | | | | | | | | | | |
|---------------|------------------|--------|------|---------------------------|-------------|-------------|-------------|-------------|-------------|-------------|-------------|-------------|-------------|-------------|-------------|
| | prec. | recall | IoU | ceil. | floor | wall | win. | chair | bed | sofa | table | tvs | furn. | objs. | avg. |
| 3DRecGAN [46] | - | - | 72.1 | 79.9 | 75.2 | 48.2 | 28.9 | 20.2 | 64.4 | 54.6 | 25.7 | 17.4 | 33.7 | 24.4 | 43.0 |
| SSCNet [32] | 76.3 | 95.2 | 73.5 | 96.3 | 84.9 | 56.8 | 28.2 | 21.3 | 56.0 | 52.7 | 33.7 | 10.9 | 44.3 | 25.4 | 46.4 |
| ForkNet [40] | - | - | 86.9 | 95.0 | 85.9 | 73.2 | 54.5 | 46.0 | 81.3 | 74.2 | 42.8 | 31.9 | 63.1 | 49.3 | 63.4 |
| SATNet [20] | 80.7 | 96.5 | 78.5 | 97.9 | 82.5 | 57.7 | 58.5 | 45.1 | 78.4 | 72.3 | 47.3 | 45.7 | 67.1 | 55.2 | 64.3 |
| VVNet [10] | 90.8 | 91.7 | 84.0 | 98.4 | 87.0 | 61.0 | 54.8 | 49.3 | 83.0 | 75.5 | 55.1 | 43.5 | 68.8 | 57.7 | 66.7 |
| SGCNet [48] | 92.6 | 90.4 | 84.5 | 96.6 | 83.7 | 74.9 | 59.0 | 55.1 | 83.3 | 78.0 | 61.5 | 47.4 | 73.5 | 62.9 | 70.5 |
| CCPNet [49] | 98.2 | 96.8 | 91.4 | 99.2 | 89.3 | 76.2 | 63.3 | 58.2 | 86.1 | 82.6 | 65.6 | 53.2 | 76.8 | 65.2 | 74.2 |
| Our Results | 92.1 | 95.5 | 88.1 | 98.2 | 92.8 | 76.3 | 61.9 | 62.4 | 87.5 | 80.5 | 66.3 | 55.2 | 74.6 | 67.8 | 74.8 |

Table 2: Quantitative comparison on the SUNCG dataset. The evaluation metric is Intersection over Union (IoU). Better results are in bold font. Our method outperforms other state-of-art methods on the average IoU.

4.2. Semantic scene completion from a depth image

The goal is to predict the occupancy and semantic labels in the view frustum for single depth images of indoor scenes.

Dataset We use the SUNCG dataset provided by [32]. The training/testing dataset contains 150k/470 depth images and the corresponding ground-truth label volumes. We convert the depth images to point clouds with normals and build octrees with depth 8. The resolution of the ground-truth volumes is $60 \times 36 \times 60$, we convert the non-empty voxels to point clouds with labels, and build octrees with depth 6.

Implementation details We use the intersection over union (IoU) between the predicted voxels and the ground-truth voxels as the evaluation metric. In our network, we set $n = 3$ for $Resblock(n, c)$. Since the network in Figure 1 takes the octree of depth 6 as input while the depth of octree is 8 in this experiment, we add the following O-CNN blocks to process and downsample the signal:

$$\begin{aligned} \text{input} &\rightarrow conv(3, 1, 16) \rightarrow pooling \rightarrow conv(3, 1, 16) \\ &\rightarrow Resblock(32, 1) \rightarrow conv(2, 2, 64) \end{aligned}$$

In total, the network layer depth is 72. The training details are provided in supplementary materials.

Comparison We validate the effectiveness of our method and compare it with state-of-the-art methods: 3DRecGAN [46], ForkNet [40], SSCNet [32], SATNet [20], VVNet [10], SGCNet [48] and CCPNet [49]. Among them, SGCNet [49] shares some similarities with our network, which is also based on U-Net and uses the sparse convolution [9] in the encoder. However, SGCNet’s decoder is based on volumetric CNNs.

For simplicity, we did not balance the training data as [32, 48, 49] have done or use the average voting trick as [10, 49] have used, although these tricks are known to improve the network performance. The evaluation results are summarized in Table 2. Our method achieves the best results on the average IoU metric in semantic scene completion.

We did a simple ablation study on this task. First, we use 2 Resblocks and reduce the network depth to 54 (with a similar amount of parameters and network depth to SGCNet), the average IoU of semantic scene completion drops from 74.2% to 70.9%; Second, we train the network without the output-guided skip connections, and the IoU drops from 74.8% to 49.3%. The ablation study proves the importance of using deep layers and output-guided skip connections.

Visual results The complete scenes by our method are illustrated in Figure 6. The output is in the voxelized representation and the colors represent different semantic labels. Here we also compare the results of VVNet and SSCNet whose implementation is available to the public. Our results are clearly much more faithful to the ground-truth than the competitive methods.

5. Conclusion

We proposed simple yet effective octree-based networks for shape and scene completion. Our network achieves significant improvements in prediction accuracy, with the aid of our output-guided skip connections and the very deep octree-based network structures. Experiments well demonstrate that our network outperforms the state-of-the-art work.

A. Acknowledgements

We wish to thank the anonymous reviewers for their constructive feedback, Chun-Yu Sun and Yu-Xiao Guo for preparing the dataset.

B. Discussions

Comparison to implicit function-based approaches Recently, implicit functions are used in deep learning as the 3D shape representation [3, 21, 22]. We did not conduct experiments to compare with these methods since they are *orthogonal* to our method: they focus on the shape representation whereas we focus on network structures. Technically, DeepSDF [22] was applied to shape completion by optimizing the latent code to match the partial data while completing the missing part, per shape, in a computationally expensive and memory-costly way. Our method can directly output the shape in one single forward pass. OccNet [21] uses the autoencoder architecture directly without skip-connection, the partial input cannot be well preserved. IM-Net [3] has not been tested the completion task.

Ablation study on skip connections l_2 and l_3 in Figure 2 3DEPN is based on a dense U-Net and the decoder of SGCNet is also a dense network. We regard them as comparable dense networks and do the comparisons with similar amount of parameters and network depth in Section 4. 3DEPN and SGCNet use full skip-connections, including l_2 and l_3 . In the ablation studies, our network without l_2 and l_3 achieves better results.

C. Training details for the experiments

For the experiments in Section 4.1 and 4.2, we use the same set of training parameters. Specifically, we set the batch size to 8 and the weight decay to 0.0005, use stochastic gradient descent (SGD) with a momentum of 0.9. The initial learning rate is set as 0.1 and decreases by a factor of 10 after about 6 epochs. The training process stops after 25 epochs.

D. Shape reconstruction from a meso-skeleton

To demonstrate the flexibility of the proposed method, we also conduct experiment on the task of reconstructing a complete 3D shape from its meso-skeleton.

Dataset We use the chair and plane datasets provided by [47], which include the synthesized meso-skeletons and the corresponding 3D shapes. The chair dataset contains 889 training and 100 testing pairs, and the airplane dataset contains 626 training and 100 testing pairs. The meso-skeletons are represented as point cloud containing 2048 points, with which we build the octree directly. For the 3D shapes, we use the virtual scanner to convert them into dense point cloud

with oriented normals [38], then build the target octrees. The depth of octree is set as 6. The two datasets are trained *separately*, which is the same as P2P-NET.

Implementation details We use the same network as the one used in shape completion. To avoid overfitting, we rotate each skeleton and the corresponding ground-truth object along with the upright axis 12 times for data augmentation. The batch size is set as 24, and the network is trained using SGD with a momentum of 0.9 and a weight decay of 0.0005. The initial learning rate is set as 0.1 and decreases by a factor of 2 after 60 epochs. The training process stops after 120 epochs. We use the Chamfer distance defined in as the evaluation metric.

Comparison We do a comparison with P2P-Net [47]. Since there is no explicit point correspondence between the meso-skeleton and the target shape, P2P-Net relies on a loss function enforcing a shape-wise similarity between the predicted and the target point sets during the training stage to build the correspondence. We directly build the correspondence between the input meso-skeleton and output shape with the proposed skip connections. On the dataset plane and chair, the medians of Chamfer distances are 1.04 and 5.55 for our methods, 1.66 and 6.06 for P2P-Net.

Visual results The visual results are shown in Figure 7. Compared with P2P-Net, the point clouds produced by our method are regularly distributed. Since the point normal is also regressed with the loss function, the output point cloud can be directly used as the input of the Poisson Reconstruction method. The reconstructed meshes are shown in the fourth column of Figure 7. However, it is very hard and even impossible to reconstruct surface mesh from the point cloud of P2P-Net, since the point cloud of P2P-Net is scattered and the internal volume structure of the shape is not kept, which makes it extremely difficult to define the inside and outside for the shape.

References

- [1] F. Calakli and G. Taubin. SSD: Smooth signed distance surface reconstruction. *Comput. Graph. Forum*, 30(7), 2011. 1
- [2] Yan-Pei Cao, Zheng-Ning Liu, Zheng-Fei Kuang, Leif Kobbelt, and Shi-Min Hu. Learning to reconstruct high-quality 3D shapes with cascaded fully convolutional networks. In *European Conference on Computer Vision (ECCV)*, 2018. 2
- [3] Zhiqin Chen and Hao Zhang. Learning implicit fields for generative shape modeling. In *Computer Vision and Pattern Recognition (CVPR)*, 2019. 2, 7
- [4] Brian Curless and Marc Levoy. A Volumetric Method for Building Complex Models from Range Images. In *SIGGRAPH*, 1996. 4

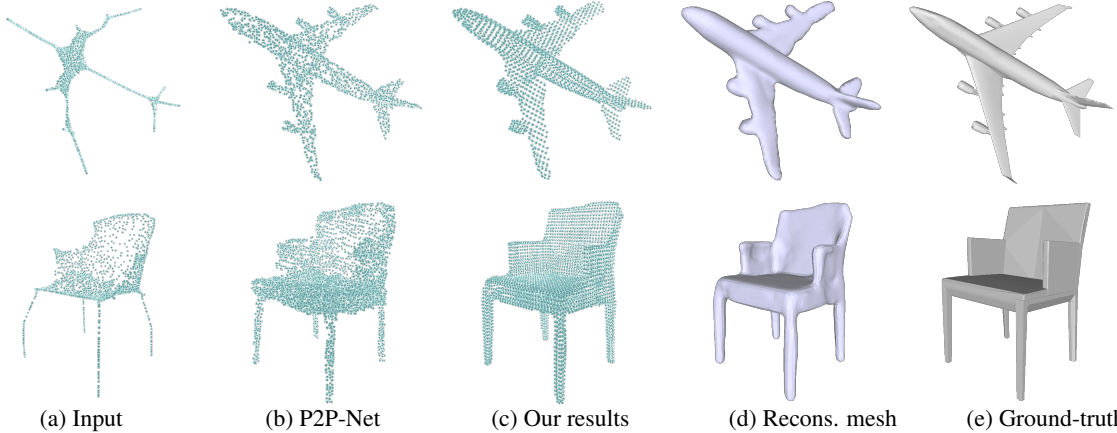


Figure 7: Visual results of shape reconstruction from meso-skeletons. Compared with P2P-Net, the point cloud of our method is regularly distributed. And since the normal is also regressed, the complete meshes can be reconstructed, which is hard or even impossible for the point clouds of P2P-Net.

- [5] Angela Dai, Charles Ruizhongtai Qi, and Matthias Niessner. Shape completion using 3D-encoder-predictor CNNs and shape synthesis. In *Computer Vision and Pattern Recognition (CVPR)*, 2017. 1, 2, 4
- [6] Angela Dai, Daniel Ritchie, Martin Bokeloh, Scott Reed, Jürgen Sturm, and Matthias Nießner. ScanComplete: Large-Scale Scene Completion and Semantic Segmentation for 3D Scans. In *Computer Vision and Pattern Recognition (CVPR)*, 2018. 1
- [7] Michael Firman, Oisin Mac Aodha, Simon Julier, and Gabriel J. Brostow. Structured prediction of unobserved voxels from a single depth image. In *Computer Vision and Pattern Recognition (CVPR)*, 2016. 2
- [8] Ian Goodfellow, Yoshua Bengio, and Aaron Courville. *Deep Learning*. MIT Press, 2016. 1
- [9] Benjamin Graham and Laurens van der Maaten. Sub-manifold Sparse Convolutional Networks. *arXiv preprint arXiv:1706.01307*, 2017. 2, 6
- [10] Yuxiao Guo and Xin Tong. View-volume network for semantic scene completion from a single depth image. In *IJCAI*, 2018. 2, 6
- [11] Xiaoguang Han, Zhen Li, Haibin Huang, Evangelos Kalogerakis, and Yizhou Yu. High-resolution shape completion using deep neural networks for global structure and local geometry inference. In *International Conference on Computer Vision (ICCV)*, 2017. 1, 2
- [12] Christian Häne, Shubham Tulsiani, and Jitendra Malik. Hierarchical surface prediction for 3D object reconstruction. In *Proc. Int. Conf. on 3D Vision (3DV)*, 2017. 2
- [13] Gur Harary, Ayellet Tal, and Eitan Grinspun. Context-based Coherent Surface Completion. *ACM Trans. Graph.*, 33(1), 2014. 2
- [14] K. He, X. Zhang, S. Ren, and J. Sun. Deep residual learning for image recognition. In *Computer Vision and Pattern Recognition (CVPR)*, 2016. 1, 2
- [15] Kaiming He, Xiangyu Zhang, Shaoqing Ren, and Jian Sun. Identity mappings in deep residual networks. In *European Conference on Computer Vision (ECCV)*, 2016. 2
- [16] Krzysztof Kaczmarski and Paweł Rzazewski. Thrust and CUDA in data intensive algorithms. In *New Trends in Databases and Information Systems*, 2013. 3
- [17] Michael Kazhdan, Matthew Bolitho, and Hugues Hoppe. Poisson surface reconstruction. In *Symp. Geom. Proc. Eurographics Association*, 2006. 1, 2
- [18] Michael Kazhdan and Hugues Hoppe. Screened Poisson surface reconstruction. *ACM Trans. Graph.*, 32(3), 2013. 2, 5
- [19] Roman Klokov and Victor Lempitsky. Escape from cells: Deep Kd-networks for the recognition of 3D point cloud models. In *International Conference on Computer Vision (ICCV)*, 2017. 2
- [20] Shice Liu, Yu Hu, Yiming Zeng, Qiankun Tang, Beibei Jin, Yinhe Han, and Xiaowei Li. See and think: Disentangling semantic scene completion. In *Neural Information Processing Systems (NeurIPS)*, 2018. 1, 6
- [21] Lars Mescheder, Michael Oechsle, Michael Niemeyer, Sebastian Nowozin, and Andreas Geiger. Occupancy networks: Learning 3d reconstruction in function space. In *Computer Vision and Pattern Recognition (CVPR)*, 2019. 2, 7
- [22] Jeong Joon Park, Peter Florence, Julian Straub, Richard Newcombe, and Steven Lovegrove. DeepSDF: Learning continuous signed distance functions for shape representation. In *Computer Vision and Pattern Recognition (CVPR)*, 2019. 2, 7
- [23] Charles R. Qi, Hao Su, Kaichun Mo, and Leonidas J. Guibas. PointNet: Deep learning on point sets for 3D classification and segmentation. In *Computer Vision and Pattern Recognition (CVPR)*. IEEE, 2017. 2
- [24] Charles Ruizhongtai Qi, Hao Su, Matthias Nießner, Angela Dai, Mengyuan Yan, and Leonidas J. Guibas. Volumetric and multi-view CNNs for object classification on 3D data. In *Computer Vision and Pattern Recognition (CVPR)*, 2016. 5
- [25] Charles R Qi, Li Yi, Hao Su, and Leonidas J Guibas. PointNet++: Deep hierarchical feature learning on point sets in a metric space. In *Neural Information Processing Systems (NeurIPS)*, 2017. 2

- [26] Gernot Riegler, Ali Osman Ulusoy, Horst Bischof, and Andreas Geiger. OctNetFusion: Learning depth fusion from data. In *Proc. Int. Conf. on 3D Vision (3DV)*, 2017. 2, 3
- [27] Gernot Riegler, Ali Osman Ulusoy, and Andreas Geiger. OctNet: Learning deep 3D representations at high resolutions. In *Computer Vision and Pattern Recognition (CVPR)*. IEEE, 2017. 2, 3
- [28] Olaf Ronneberger, Philipp Fischer, and Thomas Brox. U-Net: Convolutional networks for biomedical image segmentation. In *International Conference on Medical image computing and computer-assisted intervention*, pages 234–241, 2015. 1, 2
- [29] Tianjia Shao, Weiwei Xu, Kun Zhou, Jingdong Wang, Dongping Li, and Baining Guo. An Interactive Approach to Semantic Modeling of Indoor Scenes with an RGBD Camera. *ACM Trans. Graph. (SIGGRAPH ASIA)*, 31(6), 2012. 1, 2
- [30] Andrei Sharf, Marc Alexa, and Daniel Cohen-Or. Context-based Surface Completion. *ACM Trans. Graph. (SIGGRAPH)*, 23(3), 2004. 2
- [31] Chao-Hui Shen, Hongbo Fu, Kang Chen, and Shi-Min Hu. Structure Recovery by Part Assembly. *ACM Trans. Graph. (SIGGRAPH ASIA)*, 31(6), 2012. 1, 2
- [32] Shuran Song, Fisher Yu, Andy Zeng, Angel X Chang, Manolis Savva, and Thomas Funkhouser. Semantic scene completion from a single depth image. In *Computer Vision and Pattern Recognition (CVPR)*, 2017. 1, 2, 6
- [33] David Stutz and Andreas Geiger. Learning 3D shape completion from laser scan data with weak supervision. In *Computer Vision and Pattern Recognition (CVPR)*. IEEE Computer Society, 2018. 2
- [34] Hao Su, Haoqiang Fan, and Leonidas Guibas. A point set generation network for 3D object reconstruction from a single image. In *Computer Vision and Pattern Recognition (CVPR)*, 2017. 2
- [35] Minhyuk Sung, Vladimir G Kim, Roland Angst, and Leonidas Guibas. Data-driven structural priors for shape completion. *ACM Trans. Graph. (SIGGRAPH ASIA)*, 34(6), 2015. 2
- [36] Andrea Tagliasacchi, Matt Olson, Hao Zhang, Ghassan Hamarneh, and Daniel Cohen-Or. VASE: Volume-Aware Surface Evolution for Surface Reconstruction from Incomplete Point Clouds. *Computer Graphics Forum*, 30(5), 2011. 1
- [37] M. Tatarchenko, A. Dosovitskiy, and T. Brox. Octree generating networks: efficient convolutional architectures for high-resolution 3D outputs. In *International Conference on Computer Vision (ICCV)*, 2017. 2
- [38] Peng-Shuai Wang, Yang Liu, Yu-Xiao Guo, Chun-Yu Sun, and Xin Tong. O-CNN: Octree-based convolutional neural networks for 3D shape analysis. *ACM Trans. Graph. (SIGGRAPH)*, 36(4), 2017. 1, 2, 7
- [39] Peng-Shuai Wang, Chun-Yu Sun, Yang Liu, and Xin Tong. Adaptive O-CNN: A patch-based deep representation of 3D shapes. *ACM Trans. Graph. (SIGGRAPH ASIA)*, 2018. 1, 2, 4
- [40] Yida Wang, David Joseph Tan, Nassir Navab, and Federico Tombari. ForkNet: Multi-branch volumetric semantic completion from a single depth image. In *International Conference on Computer Vision (ICCV)*, 2019. 1, 6
- [41] Jane Wilhelms and Allen Van Gelder. Octrees for faster isosurface generation. *ACM Trans. Graph.*, 11(3), 1992. 3
- [42] Jiajun Wu, Chengkai Zhang, Tianfan Xue, William T. Freeman, and Joshua B. Tenenbaum. Learning a probabilistic latent space of object shapes via 3D generative-adversarial modeling. In *Neural Information Processing Systems (NeurIPS)*, 2016. 2
- [43] Jiajun Wu, Chengkai Zhang, Xiuming Zhang, Zhoutong Zhang, William T Freeman, and Joshua B Tenenbaum. Learning shape priors for single-view 3D completion and reconstruction. In *European Conference on Computer Vision (ECCV)*, 2018. 1
- [44] Q. Wu, K. Xu, and J. Wang. Constructing 3D CSG models from 3D raw point clouds. *Comput. Graph. Forum*, 37(5), 2018. 2
- [45] Z. Wu, S. Song, A. Khosla, F. Yu, L. Zhang, X. Tang, and J. Xiao. 3D ShapeNets: A deep representation for volumetric shape modeling. In *Computer Vision and Pattern Recognition (CVPR)*. IEEE, 2015. 2
- [46] Bo Yang, Stefano Rosa, Andrew Markham, Niki Trigoni, and Hongkai Wen. Dense 3D object reconstruction from a single depth view. *IEEE Trans. Pattern Anal. Mach. Intell.*, 2018. 1, 2, 4, 6
- [47] Kangxue Yin, Hui Huang, Daniel Cohen-Or, and Hao Zhang. P2P-NET: Bidirectional Point Displacement Net for Shape Transform. *ACM Trans. Graph. (SIGGRAPH)*, 37(4), 2018. 7
- [48] Jiahui Zhang, Hao Zhao, Anbang Yao, Yurong Chen, Li Zhang, and Hongen Liao. Efficient semantic scene completion network with spatial group convolution. In *European Conference on Computer Vision (ECCV)*, 2018. 2, 6
- [49] Pingping Zhang, Wei Liu, Yinjie Lei, Huchuan Lu, and Xiaoyun Yang. Cascaded context pyramid for full-resolution 3D semantic scene completion. In *International Conference on Computer Vision (ICCV)*, 2019. 1, 6
- [50] Bo Zheng, Yibiao Zhao, Joey C. Yu, Katsushi Ikeuchi, and Song-Chun Zhu. Beyond Point Clouds: Scene Understanding by Reasoning Geometry and Physics. In *Computer Vision and Pattern Recognition (CVPR)*, 2013. 2
- [51] Kun Zhou, Minmin Gong, Xin Huang, and Baining Guo. Data-parallel octrees for surface reconstruction. *IEEE. T. Vis. Comput. Gr.*, 17(5), 2011. 3